LWT - Food Science and Technology 197 (2024) 115902

Contents lists available at ScienceDirect

LWT

journal homepage: www.elsevier.com/locate/lwt

Influence of temperature on 'Rojo Brillante' persimmon drying. Quality characteristics and drying kinetics

Lourdes Cervera-Chiner[a,c,1,*], Nariane Q. Vilhena[a,1], Virginia Larrea[b], Gemma Moraga[b], Alejandra Salvador[a]

[a] *Postharvest Department, Instituto Valenciano de Investigaciones Agrarias, 46113, Valencia, Spain*

[b] *Food Microstructure and Chemistry Research Group (MIQUALI), Instituto Universitario de Ingeniería de Alimentos-FoodUPV, Universitat Politècnica de València, Valencia, Spain*

[c] *Instituto Universitario de Ingeniería de Alimentos-FoodUPV, Universitat Politècnica de València, Valencia, Spain*

ARTICLE INFO

Keywords:
Dried persimmon
Hot-air drying
Texture
Secondary epidermis
Microstructure

ABSTRACT

A physico-chemical characterization and drying kinetics study was performed for whole 'Rojo Brillante' persimmon subjected to hot-air drying at 35 °C, 40 °C and 45 °C. Fruit was dried until a moisture content of 30 g water/100 g product, which is required to be considered dried persimmon. This moisture value was obtained after 12, 8 and 7 d when the drying process was applied at 35 °C, 40 °C and 45 °C, respectively. All the drying treatments caused flesh structure changes, shrinkage and secondary epidermis formation. The final product's quality characteristics especially the texture, strongly depended on drying temperature. The fruit dried at 35 °C exhibited a gelatinous internal texture and a thin secondary epidermis, similarly to that obtained during a natural drying process. The drying treatment at 40 °C resulted in fruit having more rubbery flesh. However, the fruit dried at 45 °C had a corky texture, with a very thick secondary epidermis that resulted in excessively tough fruit for commercialization purposes. The differences in flesh structure were revealed in the microstructural study by Cryo-FESEM. In all cases, soluble tannins content lowered to non-astringency values. Hot-air drying technology proved to be a good alternative to valorize discarded 'Rojo Brillante' persimmon.

1. Introduction

Persimmon (*Diospyros kaki* Thunb.) is a crop of Chinese origin that has become one of the most important cultures in the Mediterranean region of Spain, with an annual production of approximately 500,000 tons, which centers mainly on the astringent cultivar Rojo Brillante (Mañez, 2019; Morales, Rodríguez-Carretero, Martínez-Alcántara, Canet, & Quiñones, 2022). High persimmon production associated with a short harvesting season has led to an increase in postharvest losses, which can reach up to 30 % of total production (Fernandez-Zamudio, Barco & Schneider, 2020). Therefore, the development of value-added by-products emerges as a strategy to reduce fruit waste and to valorize surplus persimmon production (Igual, Castelló, Roda, & Ortolá, 2011).

Drying is one of the oldest fruit preservation methods that prolongs shelf life and enables fruit consumption during all seasons (Doymaz, 2012). Most studies carried out so far are focused on drying of sliced persimmon (Igual et al., 2011; Senadeera, Adiletta, Önal, Di Matteo, & Russo, 2020; Llorca, Pons-Gomez & Besada, 2023; Zhao, Amer & Eun, 2021). Nevertheless, in Asian countries, whole fruit drying is a traditional technique used for persimmon (Hur, Kang, Lee, Lee, & Lee, 2014; Jia, Katsuno & Nishizu, 2019). The drying of whole persimmon has been characterized for some cultivars such as Fuyu (Khaliq et al., 2022), Triumph (Park et al., 2006), Sanggandungsi (Cho et al., 2017) and a persimmon variety produced in Turkey (Demiray & Tulek, 2017). Although the whole persimmon drying technology has not yet been implemented in Spain and other production areas, recent studies have revealed that cv. Rojo Brillante is suitable for being submitted to natural-air drying processes (González, Gil, Moraga, & Salvador, 2021; Vilhena, Gil, Llorca, Moraga, & Salvador, 2020). Drying is also reported to eliminate 'Rojo Brillante' astringency due to tannins insolubilization, with the water loss process being an interesting aspect to allow its commercialization without the need for postharvest deastringency

* Corresponding author. Postharvest Department, Instituto Valenciano de Investigaciones Agrarias (IVIA), Ctra. Moncada-Náquera CV-315, Km 10.7, 46113, Moncada, Spain.

E-mail address: loucerch@upv.edu.es (L. Cervera-Chiner).

[1] The first two authors contributed equally to this manuscript.

https://doi.org/10.1016/j.lwt.2024.115902
Received 8 November 2023; Received in revised form 25 January 2024; Accepted 26 February 2024
Available online 3 March 2024

treatment (Matsumoto et al., 2007).

Dried persimmon can be classified into dried and semi-dried based on its water content, and the moisture limit for this classification is variable among countries and varieties (Choi et al., 2017). In South Korea, which is one of the main dried persimmon producing countries, the final water content is 50 g water/100 g product for semi-dried and 30 g water/100 g product for dried fruit. The period to achieve this moisture by natural-air drying lasts between approximately 25 and 60 d (Kang et al., 2004; Kim, Chung, Kim, & Kim, 2018; Lee, Moon, Lee, & Kim, 2011). For cv. Rojo Brillante, Vilhena et al. (2020) achieved a water content of 50 g water/100 g product at 25 drying d and 30 g water/100 g product at 50 drying d.

However, the long time required to reach the desired moisture content, and the fact that fruit can be contaminated by airborne spores during the process, are some drawbacks for implementing natural-air drying on an industrial scale (Cárcel, García-Pérez, Riera, & Mulet, 2007). In addition, it does not seem to be a suitable technique for regions with high relative humidity and warm temperatures like the Spanish Mediterranean region. Therefore, strategies are being sought to improve the drying process. Hot-air drying appears to be a good solution to shorten the procedure without losing final product quality, as shown for different fruit crops like grapes (Adiletta, Russo, Senadeera, & Di Matteo, 2016), plums (Hedatizadeh & Chaji, 2016) and dates (Falade & Abbo, 2007), and for different persimmon cultivars produced in Asia (Demiray & Tulek, 2017; Jia, Katsuno, & Nishizu, 2020; Sugiura & Taira, 2009).

Studies have proposed different mathematical models to describe the drying process in fruit such as peach (Kingsly, Goyal, Manikantan, & Ilyas, 2007), apricot (Doymaz, 2004), apple (Sacilik et al., 2006), strawberry (Beltagy et al., 2007), plums (Doymaz, 2004) or black grape (Toğrul, 2010). For persimmon, González et al. (2021) have reported six mathematical models suitable for fitting the data from the natural drying process of whole fruit. Nevertheless, these models have not been evaluated for hot-air drying process.

Thus, the objective of this work is the optimization of whole fruit drying technology for 'Rojo Brillante' persimmon by applying different drying temperatures by means of evaluating fruit physico-chemical and microstructural characteristics.

2. Material and methods

2.1. Fruit samples and experimental procedure

Persimmon cv. Rojo Brillante in the commercial maturity stage was obtained from a fruit cooperative (Cooperativa Agrícola Sant Bernart Coop. V.) located in Carlet (Valencian Community, Spain). Fruit was transported to the *Instituto Valenciano de Investigaciones Agrarias (IVIA)*, where they were selected according to homogenous size, color and lack of external damage. The initial flesh firmness was 35.76 ± 4.77 N and the peel color index was 14.27 ± 4.20.

Twenty fruits were taken for the initial characterization. The rest were separated into three batches of 80 fruit to be subjected to three drying temperatures. Fruit was sanitized with sodium hypochlorite solution (1/10 v.v., for 4 min) and placed on absorbent paper to dry in the open air. Subsequently, fruit were manually peeled, individually identified and hung by the pedicel in convective drying chambers (FED 260 Standard model, Binder, Tuttlingen, Germany).

Fruit was subjected to forced air drying conditions at an air velocity of 2 m/s at 35 ºC, 40 ºC or 45 ºC. In all cases, fruit were dried until reach a moisture content of 30 ± 2 g water/100 g product on a wet basis (w.b.) according to Choi et al. (2017). The duration of the process depended on the time when fruit achieved the established moisture.

2.2. Determinations

The following physico-chemical determinations were made on eight fruit per treatment before drying (d 0) and periodically throughout the drying process until samples reached a moisture content of 30 g water/100 g product: water content, water activity (aw), diameters, epidermis thickness, color, texture, total soluble solids (TSS) and soluble tannins (ST). In addition, a microstructural study was carried out with fresh fruit and at the end of the drying process.

2.2.1. Moisture, water activity and drying kinetics

Three fruit per treatment were taken to determine the moisture and water activity (a_w). For this purpose, they were crushed individually by a crushing machine (Moulinex AD560120) and the water content of samples was analyzed by vacuum drying (Vaciotem, J.P. Selecta vacuum oven) at 60 °C to constant weight according to the standard method of AOAC (2005). The results were expressed as g water/100 g product. Water activity was determined using a dew point hygrometer device (Aqualab CX-2 Decagon). All these determinations were replicated three times.

Given the aim of characterize fruit drying behavior at the three drying temperatures, the experimental moisture data were fitted to six mathematical models previously employed for whole persimmons dried by natural air (González et al., 2021) (Table 1).

These models relate the moisture ratio (MR) to the drying time (in d). The MR is calculated from the water content of the samples by applying Equation (1):

$$MR = \left(\frac{M_i - M_e}{M_0 - M_e}\right) \quad (1)$$

where M_0 is the moisture content at the initial time, M_i is the moisture content at any drying time, and M_e is the equilibrium moisture content, which can be neglected for being relatively low. Therefore, the MR can be expressed as M_i/M_0.

The regression analysis was determined by the Solver statistical software (Excel 2016). The criteria for selecting the best model to define the drying curves were a high determination coefficient (R^2) and lower values of the chi-square (X^2), mean bias error (MBE), root-mean-square error (RMSE) and relative percent error (PE). These parameters were calculated by using Equations (2)–(5):

$$X^2 = \frac{\sum_{i=1}^{N}\left(MR_{exp,i} - MR_{pre,i}\right)^2}{N - z} \quad (2)$$

$$MBE = \frac{1}{n}\sum_{i=1}^{N}\left(MR_{pre,i} - MR_{exp,i}\right) \quad (3)$$

$$RMSE = \left[\frac{1}{n}\sum_{i=1}^{N}\left(MR_{pre,i} - MR_{exp,i}\right)^2\right]^{1/2} \quad (4)$$

$$PE\ (\%) = \frac{100}{N}\sum_{i=1}^{N}\frac{\left|MR_{exp,i} - MR_{pre,i}\right|}{MR_{exp,i}} \quad (5)$$

Table 1
Mathematical models applied to drying curves.

Empirical Model	Equation	References
Newton	$MR = \exp(-kt)$	Liu and Bakker-Arkema (1997)
Page	$MR = \exp(-kt^n)$	Page (1949)
Midilli et al.	$MR = a \exp(-kt^n) + bt$	Midilli, Kucuk, and Yapar (2002)
Logarithmic	$MR = a \exp(-kt^n) + c$	Toğrul and Pehlivan (2002)
Henderson & Pabis	$MR = a \exp(-kt)$	Wang et al. (2007)
Verma	$MR = a \exp(-kt) + (1-a) \exp(-gt)$	Verma, Bucklin, Endan, and Wratten (1985)

MR: moisture ratio; *k, n, a, g, c, b*: constants of each applied model; t: time in d (source: González et al., 2021).

where $MR_{exp,i}$ is the experimental MR, $MR_{pre,i}$ is the predicted MR, N is the number of observations and z is the number of constants.

2.2.2. Diameters and secondary epidermis thickness

Fruit longitudinal and equatorial diameters, as well as the thickness of the secondary epidermis that formed during the drying process, were assessed individually on each fruit by a pachymeter (Mitutoyo 500-267V-CDL20CP, Japan).

2.2.3. Color and texture

Fruit external color was measured individually on two opposite equatorial zones without peel. A Minolta Colorimeter (model CR-400, Ramsey, NY, USA) was used by applying a D65 illuminant and 10° standard observer. The Lightness (L*), Chroma (C*), and hue angle (h*) parameters were determined. The total color difference (ΔE) was calculated according to Equation (6):

$$\Delta E = \sqrt{(\Delta L^*)^2 + (\Delta a^*)^2 + (\Delta b^*)^2} \tag{6}$$

where ΔL^*, $\Delta a^*$and Δb^* are the difference of each parameter before and after all the drying treatments (Pathare, Opara & Al-Said, 2013).

Texture was assessed by a Texturometer Instron Universal Machine (model 4301, Instron Corp., Canton, MA, USA) using a 35-mm flat plunger and applying a compression force of 10 N along the fruit equatorial axis. Produced deformation was expressed as millimeters of deformation.

2.2.4. Soluble tannin content and total soluble solids

Three fruits per treatment were chopped into small pieces and mixed. Three samples of 5 g of material were taken to determine ST and TSS. ST were determined by the Folin-Denis method (Taira, 1995) and the results were expressed as a g soluble tannins/100 g dry weight.

For determining TSS, fruit samples were homogenized with distilled water at a 1/3 ratio (w/w) in a Polytron homogenizer (model PT 3100D, Kinematica, Switzerland). To avoid tannins interfering with the TSS measurements, their insolubilization was previously done according to Sugiura, Kataoka, and Tomana (1983). Measurements were taken in triplicate with a refractometer (Atagomod. PR1). The results were expressed as °Brix.

2.2.5. Microstructural analysis

For the microstructural study, a Cryo-field emission scanning electron microscopy (Cryo-FESEM, ZEISS ULTRA 55, Oxford Instruments, Abingdon, UK) was used to observe flesh samples. Cubes (3 mm^3) were cut from the equatorial area perpendicularly to the main axis of the persimmon flesh with a stainless-steel cutter. These cubes were then immersed into slush nitrogen (−210 °C) and transferred to a cryo-trans GeminiSEM 500 (ZEISS, Oberkochen, Germany) linked with a field emission scanning electron microscope, which operated at a temperature below −130 °C. Samples were cryofractured at −180 °C and etched at −90 °C. Samples were observed at 3 kV at a working distance of 68 mm.

2.2.6. Statistical analysis

The fruit physico-chemical data were subjected to analyses of variance (ANOVA) and multiple comparisons between means at $p \leq 0.05$, determined by the LSD test. The Statgraphics Centurion XVII.I software application was used for the statistical analysis (Manugistics Inc., Rockville, MD, USA).

3. Results and discussion

3.1. Moisture and water activity. Drying kinetics

The initial moisture content of fresh fruit was 80.5 ± 0.67 g water/100 g product, similar to the value previously reported for 'Rojo Brillante' persimmon (Vilhena et al., 2020). It continuously lowered during the drying process, which was faster the higher the drying temperature was (Fig. 1a). Moisture content around 30 g water/100 g product, which is the required value for dried persimmon, was reached at 12, 8 and 7 d when drying treatments were carried out at 35 °C, 40 °C and 45 °C, respectively.

The effect of temperature on persimmon drying has been related to a higher evaporation rate from the fruit surface at higher temperatures (Demiray & Tulek, 2017). For the cv. Rojo Brillante submitted to natural-air drying, the time required to reach a moisture content of 30 g water/100 g product was substantially longer, around 50 d (González et al., 2021; Vilhena et al., 2020).

The fresh fruit had a value of 0.98 for a_w (Fig. 1b). Throughout the drying process, a decrease occurred that was temperature-dependent. The fruit dried at 35 °C showed a steady decrease in a_w to values of 0.83 after 12 d when fruit reached 30 g water/100 g product of moisture content. The fruit dried at 40 °C showed a similar decrease as that recorded at 35 °C until d5, but this decrease became more marked from that time onward. At the end of drying, after 8 d it reached similar values to those of the fruit dried at 35 °C. The a_w reduction in the fruit at 45 °C was more pronounced, mainly from d5, with values of 0.70 on d7.

The moisture ratios calculated from the experimental water content values were represented according to the drying time and fitted to six drying models (Table 1). Previous studies have employed these models for different products, such as apple slices (Sacilik & Elicin, 2006) and grape seeds (Roberts, Kid & Padilla-Zakour, 2008). For persimmon, they have been previously applied for slices (Sampaio et al., 2017; Senadeera et al., 2020) and for whole fruit undergoing natural-air drying (González et al., 2021).

The parameters from the six models were estimated using a nonlinear regression analysis with persimmon samples dried at the three temperatures (Table 2). The value of the k constant of all the models ranged from 0.121 to 0.704. This value was higher as the drying temperature increased. This effect of temperature on the k value has also been observed during the drying process of persimmon slices (Senadeera et al., 2020). For naturally dried persimmon, González et al. (2021) reported lower values for the k parameter, which were between 0.027 and 0.041.

The n parameter obtained values ranging from 0.789 to 0.636, and this value lowered with drying temperature increase. During natural drying, this parameter had higher values than in the present study, and ranged from 0.983 to 1.101 (González et al., 2021). Parameters a, g, c and b were similar between models and did not present any wide variations with drying temperatures changes.

In order to test goodness of fit, five statistical parameters were employed: the R^2, X^2, MSE, RMSE and PE values (Table 2). The model that best fitted the three drying processes was Verma's model because it had the highest R^2 value (>0.999) and the lowest X^2 ($<1\cdot10^{-5}$), MBE ($<1\cdot10^{-3}$), and RMSE ($<1\cdot 10^{-5}$) values. Page's and Midilli's models followed closely, and also obtained high R^2 (>0.999) values and very low X^2, MBE and RMSE parameters. The PE values varied from 1 % to 12 % for all the models assessed for the three temperatures, and Page, Midilli and Verma's models were those with lowest values, which ranged between 1 and 2 %. These results agree with those obtained for natural-air dried persimmon (González et al., 2021), where the models that best fitted were Midilli, Logarithmic, and Verma's models. Verma's model for the three drying temperatures is plotted in Fig. 2 and shows a good fit to the experimental data at each drying temperature.

The Verma's model parameters were correlated with drying air temperature by different empirical equations (linear, quadratic and exponential). The highest R^2 was obtained for the quadratic model, being the equations as follows:

$$k = -190.37 + 1.204\ T - 0.0019\ T^2 \quad R^2 = 1 \tag{7}$$

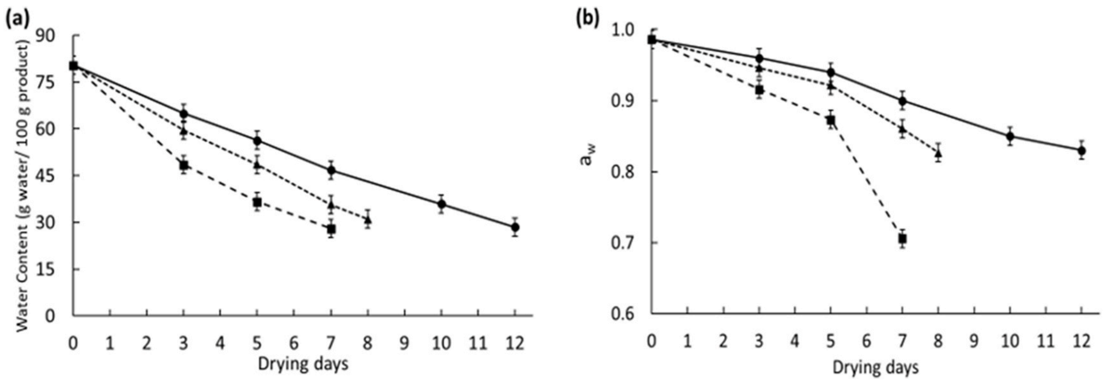

Fig. 1. Water content (a) and water activity (a_w) (b) of 'Rojo Brillante' persimmon during the drying process at 35 °C (—●—), 40 °C (--▲--) and 45 °C (– ■ –) until 30 g water/100 g product moisture was reached. The vertical bars represent Least Significant Differences (LSD) intervals ($p \leq 0.05$).

Table 2
Values of the model parameters and statistical parameters of six drying models employed for 'Rojo Brillante' persimmon dried at 35 °C, 40 °C and 45 °C.

	Model Parameters						Statistical Parameters				
Model	*k*	*n*	*a*	*g*	*c*	*b*	R^2	X^2	MBE	RMSE	PE %
35 °C											
Newton	0. 218	–	–	–	–	–	0.99	$4.1\cdot10^{-4}$	$1.2\cdot10^{-2}$	$2.7\cdot10^{-4}$	8.45
Page	0.328	0.789	–	–	–	–	0.99	$9.2\cdot10^{-6}$	$1.7\cdot10^{-3}$	$6.1\cdot10^{-6}$	0.91
Midilli et al.	0.328	0.789	1	–	–	0	0.99	$9.2\cdot10^{-6}$	$1.7\cdot10^{-3}$	$6.1\cdot10^{-6}$	0.92
Logarithmic	0.261	–	0.938	–	0.061	–	0.99	$1.7\cdot10^{-5}$	$2.4\cdot10^{-3}$	$1.1\cdot10^{-5}$	1.83
Henderson & Pabis	0.217	–	0.995	–	–	–	0.99	$4.0\cdot10^{-4}$	$1.3\cdot10^{-2}$	$2.7\cdot10^{-4}$	8.43
Verma	0.121	–	0.391	0.363	–	–	1.00	$5.4\cdot10^{-6}$	$1.4\cdot10^{-3}$	$3.6\cdot10^{-6}$	1.01
40 °C											
Newton	0.316	–	–	–	–	–	0.99	$7.9\cdot10^{-4}$	$1.8\cdot10^{-2}$	$5.3\cdot10^{-4}$	10.02
Page	0.457	0.76	–	–	–	–	0.99	$3.7\cdot10^{-5}$	$3.6\cdot10^{-3}$	$2.5\cdot10^{-5}$	1.99
Midilli et al.	0.456	0.761	1	–	–	0	0.99	$3.7\cdot10^{-5}$	$3.6\cdot10^{-3}$	$2.5\cdot10^{-5}$	1.99
Logarithmic	0.396	–	0.924	–	0.075	–	0.99	$1.5\cdot10^{-4}$	$7.0\cdot10^{-3}$	$9.8\cdot10^{-5}$	3.54
Henderson & Pabis	0.314	–	0.991	–	–	–	0.99	$7.7\cdot10^{-4}$	$1.9\cdot10^{-2}$	$5.1\cdot10^{-4}$	9.89
Verma	0.237	–	0.706	5.164	–	–	0.99	$1.4\cdot10^{-5}$	$2.1\cdot10^{-3}$	$9.4\cdot10^{-6}$	1.16
45 °C											
Newton	0.429	–	–	–	–	–	0.99	$8.3\cdot10^{-4}$	$1.7\cdot10^{-2}$	$5.5\cdot10^{-4}$	12.61
Page	0.704	0.636	–	–	–	–	0.99	$1.8\cdot10^{-5}$	$2.3\cdot10^{-3}$	$1.2\cdot10^{-5}$	1.90
Midilli et al.	0.704	0.636	1	–	–	0	0.99	$1.8\cdot10^{-5}$	$2.3\cdot10^{-3}$	$1.2\cdot10^{-5}$	1.90
Logarithmic	0.561	–	0.924	–	0.076	–	0.99	$1.0\cdot10^{-4}$	$5.6\cdot10^{-3}$	$6.9\cdot10^{-5}$	4.36
Henderson & Pabis	0.427	–	0.995	–	–	–	0.99	$8.3\cdot10^{-4}$	$1.7\cdot10^{-2}$	$5.5\cdot10^{-4}$	12.6
Verma	0.258	–	0.524	5.164	–	–	1.00	$5.0\cdot10^{-6}$	$1.1\cdot10^{-3}$	$3.3\cdot10^{-6}$	1.01

k, n, a, g, c, b: constants of each applied model.

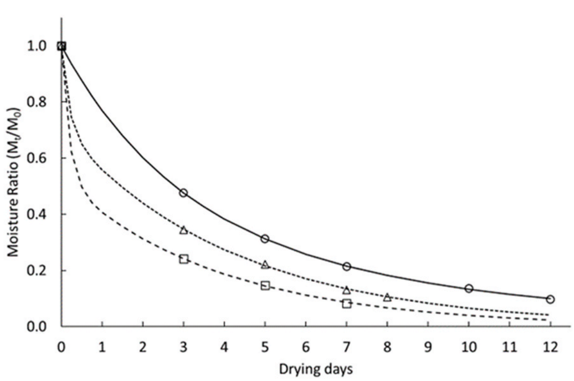

Fig. 2. Experimental data (○35 °C, △ 40 °C, □ 45 °C) and predicted (— 35 °C, ... 40 °C, --- 45 °C) drying curves using Verma's model for 'Rojo Brillante' persimmon dried at three temperatures.

$$a = -978.2 + 6.239\ T - 0.0099\ T^2 \quad R^2 = 1 \tag{8}$$

$$g = -9561.2 + 60.617\ T - 0.096\ T^2 \quad R^2 = 1 \tag{9}$$

These equations would allow us to predict the moisture content of the whole 'Rojo Brillante' persimmon during drying, at any intermediate temperature.

3.2. Physico-chemical parameters

During the drying process, a reduction in the equatorial and longitudinal diameters due to water loss and a consequent reduction in the internal volume resulted in visible fruit wrinkling (Fig. 3).

The reduction in the equatorial diameter was greater compared to the changes in the fruit longitudinal diameter (Table 3). Thus, when fruit reached a moisture content of 30 g water/100 g product, while the equatorial diameter had lowered by about 45 % in all the drying treatments, the longitudinal diameter had decreased by 19 %. The slighter reduction in the longitudinal diameter compared to the equatorial diameter was attributed to the way fruit were hung because when they were suspended by the peduncle. So, the force of gravity caused fruit to stretch downwardly, with the consequent maintenance of longitudinal size.

The reduction in fruit overall volume, defined as shrinkage, is a physical phenomenon that occurs during the dehydration process affects textural quality (Sun, Zhang, Mujumdar, & Yu, 2022). Shrinkage depends on moisture content, but also on other many factors, including material characteristics, microstructure, mechanical properties and process conditions (Mahiuddin, Khan, Kumar, Rahman, & Karim, 2018).

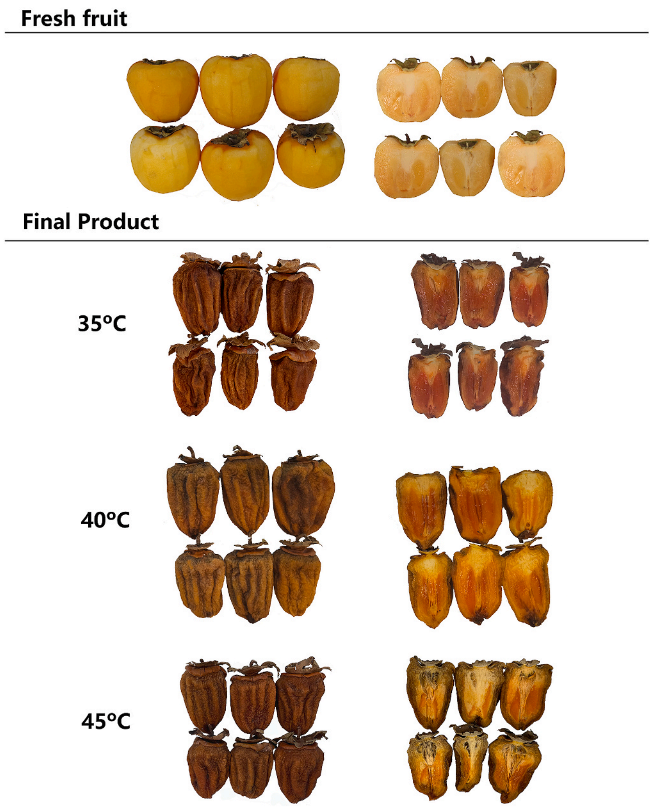

Fig. 3. Appearance of 'Rojo Brillante' persimmon in the initial stage and at the end of each drying process at 35 °C (12 d), 40 °C (8 d) and 45 °C (7 d).

Table 3
Longitudinal and equatorial diameters of persimmon 'Rojo Brillante' before (fresh fruit) and after drying until reaching a moisture content of 30 g water/100 g product at 35 °C, 40 °C or 45 °C.

		Longitudinal diameter (mm)	Equatorial diameter (mm)
Fresh fruit		77.76 ± 0.87 ^{a}	76.93 ± 0.97 ^{a}
After drying	**35 °C**	62.64 ± 1.5 ^{b}	38.80 ± 0.97 ^{b}
	40 °C	63.22 ± 1.25 ^{b}	42.81 ± 1.64 ^{b}
	45 °C	62.25 ± 1.30 ^{b}	41.47 ± 1.57 ^{b}

Different letters in the same column show significant differences according to the LSD test ($p \leq 0.05$).

In the present study, slight visual differences were observed in fruit wrinkling for the fruit subjected to the three drying temperatures, which was slightly more pronounced in the fruit dried at the lowest temperature (Fig. 3).

The drying process in persimmon has also been reported to cause fruit darkening (Çelen, 2019; Yamada, Ando, Tsutani, Amano, & Yamamoto, 2009). Flesh browning is a result of several biochemical reactions, such as degradation of carotenoids and other pigments, enzymatic and non-enzymatic reactions, as well as the oxidative and non-oxidative breakdown of ascorbic acid (Yamada et al., 2009). In the present study, fruit color was influenced by drying temperature. When fruit reached a moisture content of 30 g water/100 g product, the fruit dried at 35 °C had darker peel than that dried at 45 °C, and the fruit dried at 40 °C displayed the palest color (Fig. 3). These differences among drying temperatures were reflected in the Lightness (L*), Chroma (C*), hue angle (h*) and total color difference (ΔE) values (Table 4). Thus, the fruit dried at 35 °C had the lowest L*, C* and h* values, which indicated more fruit darkening. By considering the color changes previously reported for the natural drying of 'Rojo Brillante' persimmon, the fruit

Table 4
Color parameters (lightness-L*, Chroma-C*, Hue angle-h* and total color difference-ΔE) of persimmon 'Rojo Brillante' before (fresh fruit) and after drying at 35 °C, 40 °C or 45 °C until a moisture content of 30 g water/100 g product was reached.

		L*	C*	h*	ΔE*
Fresh fruit		71.7 ± 2.6 ^{a}	52.2 ± 0.8 ^{a}	83.9 ± 3.8 ^{a}	–
After drying	35 °C	32.9 ± 4.2 ^{d}	31.5 ± 1.6 ^{d}	53.6 ± 2.9 ^{c}	48.0 ± 4.7 ^{a}
	40 °C	43.5 ± 3.6 ^{b}	43.4 ± 1.6 ^{b}	61.4 ± 2.6 ^{b}	31.9 ± 2.4 ^{b}
	45 °C	36.3 ± 3.6 ^{c}	38.6 ± 1.6 ^{c}	59.7 ± 2.9 ^{b}	43.2 ± 4 ^{c}

Different letters in the same column show significant differences according to the LSD test ($p \leq 0.05$).

dried at 40 °C was that with the most similar L*, C* and h* values when 30 g water/100 g product of moisture content was reached (Vilhena et al., 2020).

Total color difference is the deviation of the final product color from the color at the initial time (Milczarek et al., 2020). The lowest ΔE value was obtained in the fruit dried at 40 °C, which indicates a less marked color change compared to the fresh fruit and, thus, depicts less fruit darkening (Table 4). However, for the fruit dried at 35 °C, the ΔE value was 48, which implies the darkest coloration at the end of the process versus the initial values. Senadeera et al. (2020) evaluated the influence of different hot-air temperatures on the color of persimmon slices. They observed that the biggest color changes were for the fruit dried at a lower temperature, which was related to the longer time required to obtain the dried product, with consequent browning.

During the drying process, a rigid external layer formed as water loss was faster on the external fruit surface than in the internal zone. This process is called 'crust formation'. In persimmon, this layer has been referred to as secondary epidermis or secondary surface (Jia et al., 2020; Kang et al., 2004; Vilhena et al., 2020). In this study, the thickness of this secondary epidermis depended on the drying temperature (Fig. 4a). On d3, the fruit of the three treatments presented similar epidermis thickness, which was close to 1.0 mm. Nevertheless, from that time onward, no increase in secondary epidermis thickness was observed in the fruit dried at 35 °C, but it continued to thicken up to 2.85 mm by the end of drying in the fruit dried at 40 °C. Epidermis thickness dramatically increased in the fruit dried at 45 °C, with values up to 4.12 mm on d 7. An influence of drying conditions, such as temperature and drying rate, on crust formation has been reported. A slow drying rate could allow moisture migration from the inside to replenish the product surface by reducing or avoiding crust formation (Achanta & Okos, 1996; Rahman, 2008). This may explain the thinnest secondary epidermis in the fruit dried at the lowest temperature (35 °C).

Regarding fruit texture, the drying process generally causes fruit softening and crisp texture loss. However, depending on drying intensity, hardness tends to increase again due to structure compaction (Kang et al., 2004; Sosa, Salvatori, & Schebor, 2012; Vilhena et al., 2020). In our study, the deformation registered when applying a force of 10 N increased after drying. This indicated flesh fruit softening in relation to the initial fresh fruit (Fig. 4b). On drying d 3, similar fruit softening was observed at the three drying temperatures. From that point onward, the deformation values of the fruit dried at 35 °C, continued to increase until d 7, and then remained close to 11 mm until the end of the process. From d 5 onward, the fruit dried at 40 °C underwent less deformation with values up to 5.9 mm at the end of the drying process. This finding indicates flesh hardening. For the fruit dried at 45 °C, this hardening was observed from d 3, when the lowest deformation value (3.6 mm) was reached. This would be related to the marked secondary epidermis thickening on this fruit, which confers fruit rigidity, as well as tougher internal flesh.

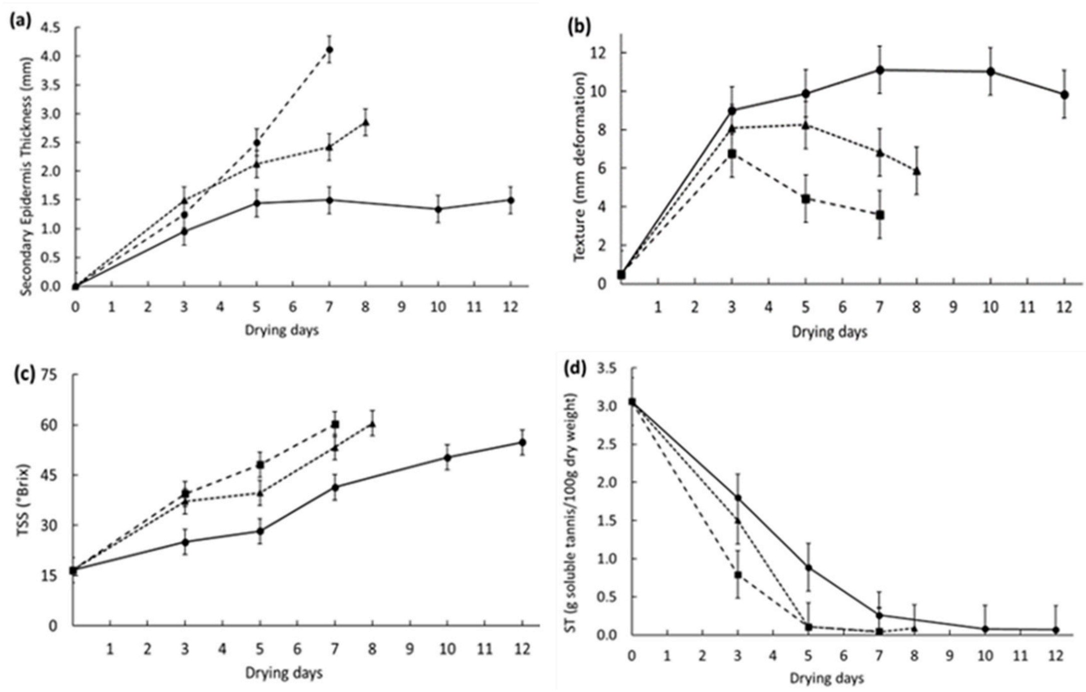

Fig. 4. Secondary epidermis thickness (a), Texture (b), Total Soluble Solids (TSS) (c) and Soluble Tannins (ST) contents (d) of 'Rojo Brillante' persimmon during the drying process at 35 °C (—●—), 40 °C (--▲--) and 45 °C (– ■ –) a moisture content of until 30 g water/100 g product was reached. The vertical bars represent Least Significant Differences (LSD) intervals ($p \leq 0.05$).

Thus, the observed internal structure was quite different depending on the drying temperature (Fig. 3). The fruit flesh dried at 35 °C showed a gel-like structure, while that of the fruit dried at 40 °C was slightly more rubbery and drier. However, the process at 45 °C resulted in a tough internal corky structure that conferred lower fruit deformation values. This structure would explain why, under these conditions, a_w was the lowest when fruit reached a moisture content of 30 g water/100 g product.

The TSS in the fresh fruit were 16.6 °Brix during persimmon drying as a result of water evaporation, and the TSS content increased (Fig. 4c). This increase in TSS at all three temperatures was concomitant with the drop in moisture that took place throughout the drying process (Fig. 1a). Drying at 40 °C and 45 °C resulted in a TSS of 60 °Brix by the time that fruit reached a moisture content of 30 g water/100 g product, while slightly lower values of 55 °Brix were obtained for the fruit dried at 35 °C. These values are similar to those reported for the natural drying of 'Rojo Brillante' (Vilhena et al., 2020).

'Rojo Brillante' persimmon is an astringent cultivar with a high tannin content at harvest (Tessmer et al., 2016; Vilhena et al., 2020). Thus, to be marketed fresh, it must undergo postharvest deastringency treatment, such as the application of ethanol or high CO_2 concentrations (Novillo, Gil, Besada, & Salvador, 2014). In some Asian countries, drying is used as a common treatment to eliminate astringency and to allow a market for astringent persimmon varieties. The time required to eliminate soluble tannins (ST) to non-astringent levels depends on both variety and drying conditions. Under natural drying conditions, 21 d are needed to completely remove 'Rojo Brillante' astringency (González et al., 2021; Vilhena et al., 2020). However, for different Japanese cultivars, fruit present no sensory astringency after 7–9 d under sun-drying conditions (Jia et al., 2020). In this study, the fresh fruit had a ST content of approximately of 3 g soluble tannins/100 g dry weight (d.b.) and this concentration dropped as drying progressed (Fig. 4d). This decline was quicker at higher drying temperatures. After 5 d, the fruit dried at 40 °C and 45 °C had ST values below to 0.3 g soluble tannins/100 g dry weight, which correspond to undetectable astringency values for 'Rojo Brillante'. However, for the fruit dried at 35 °C, these values were reached after 10 d. These results coincide with those of other authors, who have reported that astringency removal speed during drying increases with drying temperature (Manabe, Kamikawa & Tarutani, 1980).

3.3. Microstructural characterization

The microstructural study was carried out on fresh persimmon fruit and on the final product after drying at 30 °C, 40 °C and 45 °C. In all cases, a cross-section of internal persimmon flesh was observed. The fresh persimmon images show the typical flesh structure, where cells appear intact and turgid, and form a compact parenchyma (Fig. 5). Cells are rounded with small air-filled intercellular spaces. The cell membrane appears intact and surrounds each cell. The cell interior looks like a network. Previous studies have described the appearance of the ST responsible for astringency inside vacuoles of the so-called tannic cells and their insolubilization during ripening (Salvador et al., 2007; Tessmer et al., 2016). Due to moisture content, ST together with other solutes, such as sugars, are observed to form a network, which is the typical eutectic artifact caused by the water sublimation process and the immobilization of these solutes when preparing samples for Cryo-SEM observations (Hernández-Carrión, Vázquez-Gutiérrez, Hernando & Quiles, 2014). It has been reported that, when tannins are insolubilized by ripening, the eutectic artifact disappears and the interior of vacuoles looks like a compact and continuous mass (Tessmer et al., 2016).

The fresh fruit had a tannins content of approximately 3 g soluble tannins/100 g dry weight, which indicates high fruit astringency (Tessmer et al., 2016). Thus, in the Cryo-SEM images of these fruit, the cells with both ST and insoluble tannins are seen. In the images of the samples dried at different temperatures, the eutectic artifact does not form due to water loss during the drying process. Hence, it is not possible to differentiate between the cells with ST or those with insoluble tannins. Nonetheless, the results indicate complete tannin insolubilization because tannin content values dramatically dropped after the drying

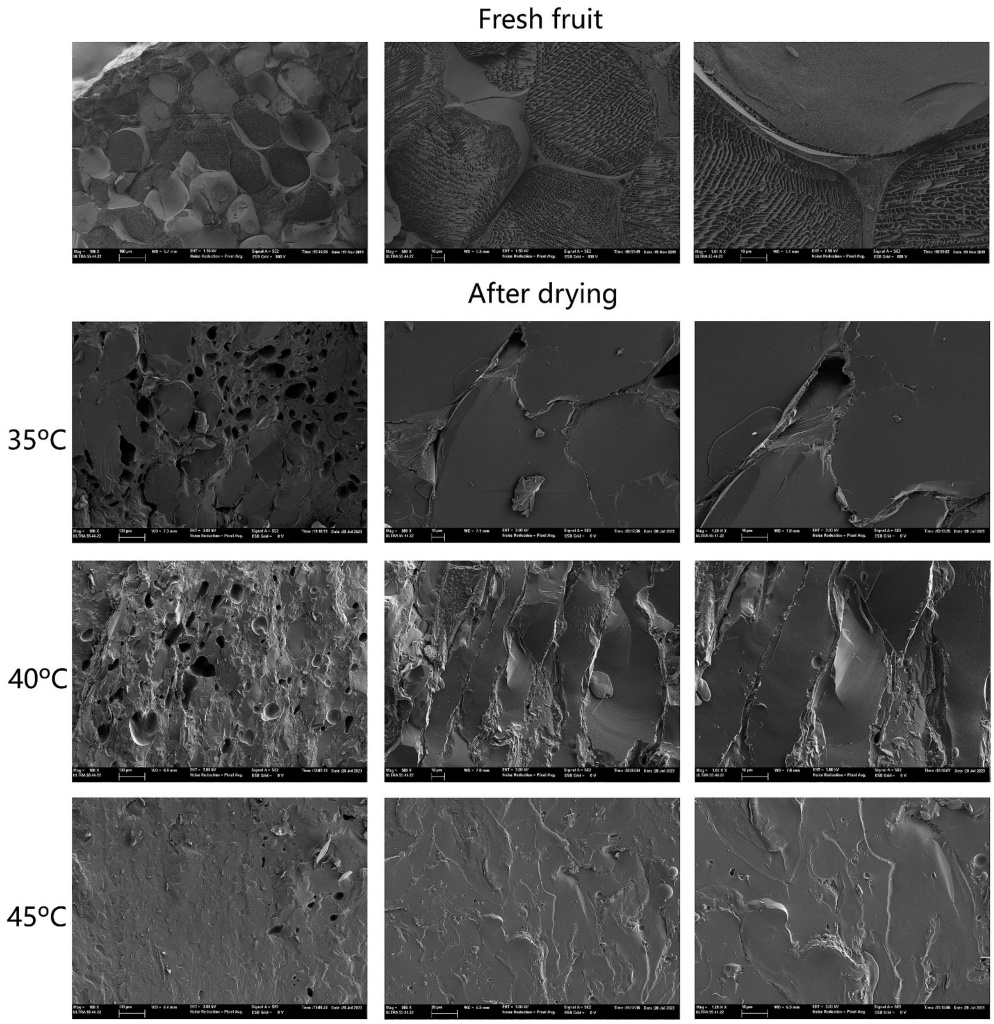

Fig. 5. Internal flesh structure by the Cryo-field emission scanning electron microscopy technique of the 'Rojo Brillante' persimmon dried until a moisture content of 30 g water/100 g product at 35 ºC, 40 ºC or 45 ºC. Magnification: 100×, 500x and 1000x.

process in all cases and reached non-astringent values, lower than 0.3 g soluble tannins/100 g dry weight (Salvador et al., 2007; Tessmer et al., 2016; Vilhena et al., 2020).

The changes in fruit flesh noted after drying at 35 ºC, 40 ºC, and 45 ºC are remarkable with evident cell structure deterioration. During drying, intracellular water transport causes cell shrinkage, pore formation and cell collapse. Finally, the overall flesh tissue is deformed due to water migration from the cell's interior (Mahiuddin et al., 2018). The images of the persimmon dried at 35 ºC reveal that cells have slightly lost their rounded shape and become somewhat elongated. This may be due to the fact that fruit have remained suspended by their peduncle and the effect of gravity can be noted. Intercellular spaces are small due to the compaction that occurs. However, the areas with pores or empty spaces are still visible. The cell membrane is no longer continuous and is much thinner than the fresh fruit. The observed structure could be related to the higher deformation values of the fruit dried at 35 ºC, and with a gel-like and more flexible appearance compared to the persimmons dried at 40 ºC and 45 ºC.

On the flesh of the fruit dried at 40 ºC, cellular compaction is greater, and these cells are no longer rounded. They have contracted and show significant elongation. Empty spaces are still observed. Cell size has also changed and become much smaller due to contraction. The cell membrane has lost its integrity and appears blurred in some areas. Even so, the cellular structure can still be distinguished, although it appears to have collapsed. This structure may justify the texture values obtained at the end of the drying process at this temperature, which are intermediate between 30 ºC and 45 ºC, and they look rubberier with a dry flesh appearance.

Finally, for the fruit dried at 45 ºC, the parenchymal structure has completely disappeared. Such parenchyma degradation is related to water removal, which occurs during drying, as observed by the Cryo-FESEM technique in previous studies (Vilhena et al., 2020). In this fruit, cells have completely lost their integrity and, therefore, no cellular organization can be distinguished. The cell membrane is practically imperceptible, and flesh has become a homogeneous, continuous and quite compact mass. This structure is consistent with the tough corky appearance of flesh (Fig. 3) and with the lowest deformation values.

4. Conclusion

The present study addresses, for the first time, the drying behavior of whole 'Rojo Brillante' persimmon that have undergone hot-air drying at 35 ºC, 40 ºC and 45 ºC. The employed mathematical models are suitable for fitting the data from the three treatments, and Verma's model is that with the best fit. The moisture content of 30 g water/100 g product required to consider dried persimmon fruit can be achieved at 12, 8, and 7 days when the drying treatment is carried out at 35 ºC, 40 ºC and 45 ºC, respectively. The final product's quality characteristics differ depending on the drying temperature, especially in texture terms. The fruit dried at 35 °C exhibited a thin secondary epidermis and a gelatinous internal texture. The drying at 40 °C resulted in fruit having more rubbery flesh, but with a similar color to that of fresh fruit. However, the fruit dried at 45 °C had a very thick secondary epidermis and a corky internal texture, which resulted in fruit being excessively hard for marketing. The microstructural study reveals parenchyma degradation and cellular structure compaction of fruit flesh for the different drying treatments. Therefore, the drying technology, may be a good strategy to increase the value of discarded fruit and to enhance the surplus of this seasonal fruit. Further research is needed to determine the appropriate packaging and storage conditions to prolong the product's shelf life.

CRediT authorship contribution statement

Lourdes Cervera-Chiner: Data curation, Formal analysis, Investigation, Writing – original draft, Writing – review & editing. **Nariane Q. Vilhena:** Data curation, Formal analysis, Investigation, Writing – original draft, Writing – review & editing. **Virginia Larrea:** Conceptualization, Data curation, Formal analysis, Investigation, Methodology, Supervision, Validation, Writing – original draft, Writing – review & editing. **Gemma Moraga:** Conceptualization, Data curation, Formal analysis, Investigation, Methodology, Supervision, Validation, Writing – original draft, Writing – review & editing. **Alejandra Salvador:** Conceptualization, Data curation, Formal analysis, Funding acquisition, Investigation, Methodology, Resources, Supervision, Validation, Writing – original draft, Writing – review & editing.

Declaration of competing interest

The authors declare that they have no known competing financial interests or personal relationships that could have appeared to influence the work reported in this paper.

Data availability

Data will be made available on request.

Acknowledgments

This research was funded by Instituto Nacional de Investigación y Tecnología Agraria y Alimentaria (INIA) and Fondo Europeo de Desarrollo Regional (FEDER), through Project RTA2017-00045-C02. The authors thank the Cooperativa Agrícola Sant Bernart Coop. V and ANECOOP for supplying the fruit herein used. L.C.C. thanks the support of the "Margarita Salas" program (2021–2024) of Universitat Politècnica de València and the Spanish Ministry of Universities, funded by the European Union-Next Generation EU (UPV Contract). N.Q.V thanks the INIA for grant FPI-INIA (PRE2018-085833).

Appendix A. Supplementary data

Supplementary data to this article can be found online at https://doi.org/10.1016/j.lwt.2024.115902.

References

Achanta, S., & Okos, M. R. (1996). Predicting the quality of dehydrated foods and biopolymers—research needs and opportunities. *Drying Technology, 14*(6), 1329–1368.

Adiletta, G., Russo, P., Senadeera, W., & Di Matteo, M. (2016). Drying characteristics and quality of grape under physical pretreatment. *Journal of Food Engineering, 172*, 9–18.

AOAC, C. (2005). *Official methods of analysis of the association of Analytical chemists international*. Gaithersburg, MD, USA: Official Methods.

Cárcel, J. A., García-Pérez, J. V., Riera, E., & Mulet, A. (2007). Influence of high-intensity ultrasound on drying kinetics of persimmon. *Drying Technology, 25*(1), 185–193.

Çelen, S. (2019). Effect of microwave drying on the drying characteristics, color, microstructure, and thermal properties of Trabzon persimmon. *Foods, 8*(2), 84.

Cho, J. H., Song, I. K., Cho, D. H., Dhungana, S. K., Ahn, H., & Kim, I. D. (2017). Quality characteristics of dried persimmon (Diospyros kaki Thunb) of different fruit sizes. *African Journal of Biotechnology, 16*(9), 429–433.

Choi, J. Y., Lee, H. J., Cho, J. S., Lee, Y. M., Woo, J. H., & Moon, K. D. (2017). Prediction of shelf-life and changes in the quality characteristics of semidried persimmons stored at different temperatures. *Food Science and Biotechnology, 26*, 1255–1262.

Demiray, E., & Tulek, Y. (2017). The effect of pretreatments on air drying characteristics of persimmons. *Heat and Mass Transfer, 53*, 99–106.

Doymaz, I. (2004a). Effect of pre-treatments using potassium metabisulphide and alkaline ethyl oleate on the drying kinetics of apricots. *Biosystems Engineering, 89*(3), 281–287.

Doymaz, I. (2004b). Effect of dipping treatment on air drying of plums. *Journal of Food Engineering, 64*(4), 465–470.

Doymaz, I. (2012). Evaluation of some thin-layer drying models of persimmon slices (Diospyros kaki L.). *Energy Conversion and Management, 56*, 199–205.

El-Beltagy, A., Gamea, G. R., & Essa, A. A. (2007). Solar drying characteristics of strawberry. *Journal of Food Engineering, 78*(2), 456–464.

Falade, K. O., & Abbo, E. S. (2007). Air-drying and rehydration characteristics of date palm (Phoenix dactylifera L.) fruits. *Journal of Food Engineering, 79*(2), 724–730.

Fernández-Zamudio, M. A., Barco, H., & Schneider, F. (2020). Direct measurement of mass and economic harvest and post-harvest losses in Spanish persimmon primary production. *Agriculture, 10*(12), 581.

González, C. M., Gil, R., Moraga, G., & Salvador, A. (2021). Natural drying of astringent and non-astringent persimmon "Rojo Brillante". Drying kinetics and physico-chemical properties. *Foods, 10*(3), 647.

Hedatizadeh, M., & Chaji, H. (2016). A review on plum drying. *Renewable and Sustainable Energy Reviews, 56*, 362–367.

Hernández-Carrión, M., Vázquez-Gutiérrez, J. L., Hernando, I., & Quiles, A. (2014). Impact of high hydrostatic pressure and pasteurization on the structure and the extractability of bioactive compounds of persimmon "Rojo Brillante". *Journal of Food Science, 79*(1), C32–C38.

Hur, S. S., Kang, B. H., Lee, D. S., Lee, S. H., & Lee, J. M. (2014). Quality characteristics of domestic dried persimmon and imported dried persimmon. *Korean Journal of Food Preservation, 21*(1), 140–145.

Igual, M., Castelló, M. L., Roda, E., & Ortolá, M. D. (2011). Development of hot-air dried cut persimmon. *International Journal of Food Engineering, 7*(5).

Jia, X., Katsuno, N., & Nishizu, T. (2019). Changes in the physico-chemical properties of persimmon (Diospyros kaki thunb.) during drying and quality deterioration during storage. *Reviews in Agricultural Science, 8*, 1–14.

Jia, X., Katsuno, N., & Nishizu, T. (2020). Effect of kneading and brushing on the physicochemical properties of "Dojo Hachiya" dried persimmon. *Food and Bioprocess Technology, 13*, 871–881.

Kang, W. W., Kim, J. K., Oh, S. L., Kim, J. H., Han, J. H., & Choi, J. U. (2004). Physicochemical characteristics of Sangju traditional dried persimmons during drying process. *Journal of the Korean Society of Food Science and Nutrition, 33*, 386–391.

Khaliq, A., Li, W. F., Ali, S., Shah, S. T., Ma, Z. H., Mao, J., et al. (2022). Thin layer drying kinetics and quality dynamics of persimmon (Diospyros kaki) treated with preservatives and solar dried under different temperatures. *PLoS One, 17*(3), Article e0265111.

Kim, J. H., Chung, I. K., Kim, H. Y., & Kim, K. M. (2018). Comparison of the quality of dried persimmon (Diospyros kaki THUNB.) treated with medicinal plant extracts and food additives. *Food Science and Nutrition, 6*(8), 1991–1998.

Kingsly, R. P., Goyal, R. K., Manikantan, M. R., & Ilyas, S. M. (2007). Effects of pretreatments and drying air temperature on drying behaviour of peach slice. *International Journal of Food Science and Technology, 42*(1), 65–69.

Lee, S. W., Moon, H. K., Lee, W. Y., & Kim, J. K. (2011). Physicochemical characteristics of cold-air dried persimmons and traditional dried persimmons. *Korean Journal of Food Preservation, 18*(4), 481–487.

Liu, Q., & Bakker-Arkema, F. W. (1997). Stochastic modelling of grain drying: Part 2. Model development. *Journal of Agricultural Engineering Research, 66*(4), 275–280.

Llorca, E., Pons-Gómez, A., & Besada, C. (2023). Physico-chemical and microstructural changes during the drying of persimmons with different disorders. Consumer acceptance of dried slices as a criterion to valorise discards. *LWT, 182*, Article 114882.

Mahiuddin, M., Khan, M. I. H., Kumar, C., Rahman, M. M., & Karim, M. A. (2018). Shrinkage of food materials during drying: Current status and challenges. *Comprehensive Reviews in Food Science and Food Safety, 17*(5), 1113–1126.

Manabe, M., Kamikawa, H., & Tarutani, T. (1980). A study of the drying Japanese persimmons III. Effects of drying temperatures on astringency removal of persimmon fruits. *Journal of the Japanese Society for Horticultural Science, 48*(4), 519–524.

Mañez, R. P. (2019). El cultivo del caqui. Antecedentes e importancia económica en España. *Distribución y Consumo, 29*(160), 44–51.

Matsumoto, T., Matsuzaki, H., Takata, K., Tsurunaga, Y., Takahashi, H., Kurahashi, T., et al. (2007). Inhibition of astringency removal in semidried Japanese persimmon fruit by 1-methylcyclopropene treatment. *HortScience, 42*(6), 1493–1495.

Midilli, A., Kucuk, H., & Yapar, Z. (2002). A new model for single-layer drying. *Drying Technology, 20*(7), 1503–1513.

Milczarek, R. R., Vilches, A. M., Olsen, C. W., Breksa, A. P., Mackey, B. E., & Brandl, M. T. (2020). Physical, microbial, and chemical quality of hot-air-dried persimmon (Diospyros kaki) chips during storage. *Journal of Food Quality, 2020*, 1–15.

Morales, J., Rodríguez-Carretero, I., Martínez-Alcántara, B., Canet, R., & Quiñones, A. (2022). DRIS norms and sufficiency ranges for persimmon 'Rojo Brillante' grown under mediterranean conditions in Spain. *Agronomy, 12*(6), 1269.

Novillo, P., Gil, R., Besada, C., & Salvador, A. (2014). Astringency removal of 'Rojo Brillante' persimmon by combining CO2 and ethanol application. *V International Conference Postharvest Unlimited, 1079*, 599–604.

Page, G. E. (1949). *Factors influencing the maximum rates of air drying shelled corn in thin layers*. Purdue University.

Park, Y. S., Jung, S. T., Kang, S. G., Licond, E. D., Ayala, A. L. M., Tapia, M. S., et al. (2006). Drying of persimmons (Diospyros kaki L.) and the following changes in the studied bioactive compounds and the total radical scavenging activities. *Lebensmittel-Wissenschaft und -Technologie, 39*(7), 748–755.

Pathare, P. B., Opara, U. L., & Al-Said, F. A. J. (2013). Colour measurement and analysis in fresh and processed foods: A review. *Food and Bioprocess Technology, 6*, 36–60.

Rahman, M. S. (2008). Post-drying aspects for meat and horticultural products. In X. D. Chen, & A. Mujumdar (Eds.), *Drying technologies in food processing* (1st ed., pp. 252–269).

Roberts, J. S., Kidd, D. R., & Padilla-Zakour, O. (2008). Drying kinetics of grape seeds. *Journal of Food Engineering, 89*(4), 460–465.

Sacilik, K., & Elicin, A. K. (2006). The thin layer drying characteristics of organic apple slices. *Journal of Food Engineering, 73*(3), 281–289.

Salvador, A., Arnal, L., Besada, C., Larrea, V., Quiles, A., & Pérez-Munuera, I. (2007). Physiological and structural changes during ripening and deastringency treatment of persimmon fruit cv. *'Rojo Brillante'. Postharvest Biology and Technology, 46*(2), 181–188.

Sampaio, R. M., Neto, J. P. M., Perez, V. H., Marcos, S. K., Boizan, M. A., & Da Silva, L. R. (2017). Mathematical modeling of drying kinetics of persimmon fruits (Diospyros kaki cv. Fuyu). *Journal of Food Processing and Preservation, 41*(1), Article e12789.

Senadeera, W., Adiletta, G., Önal, B., Di Matteo, M., & Russo, P. (2020). Influence of different hot air drying temperatures on drying kinetics, shrinkage, and colour of persimmon slices. *Foods, 9*(1), 101.

Sosa, N., Salvatori, D. M., & Schebor, C. (2012). Physico-chemical and mechanical properties of apple disks subjected to osmotic dehydration and different drying methods. *Food and Bioprocess Technology, 5*, 1790–1802.

Sugiura, A., Kataoka, I., & Tomana, T. (1983). Use of refractometer to determine soluble solids of astringent fruits of Japanese persimmon (Diospyros kaki L.). *Journal of Horticultural Science, 58*(2), 241–246.

Sugiura, A., & Taira, S. (2009). Dried persimmon production in Japan. *IV International Symposium on Persimmon, 833*, 71–76.

Sun, Q., Zhang, M., Mujumdar, A. S., & Yu, D. (2022). Research on the vegetable shrinkage during drying and characterization and control based on LF-NMR. *Food and Bioprocess Technology, 15*(12), 2776–2788.

Taira, S. (1995). Astringency in persimmon. In H. F. Linskens, & J. F. Jackson (Eds.), *Fruit analysis* (pp. 97–110). Germany: Springer.

Tessmer, M. A., Besada, C., Hernando, I., Appezzato-da-Glória, B., Quiles, A., & Salvador, A. (2016). Microstructural changes while persimmon fruits mature and ripen. Comparison between astringent and non-astringent cultivars. *Postharvest Biology and Technology, 120*, 52–60.

Toğrul, İ. T. (2010). Modelling of heat and moisture transport during drying black grapes. *International Journal of Food Science and Technology, 45*(6), 1146–1152.

Toğrul, İ. T., & Pehlivan, D. (2002). Mathematical modelling of solar drying of apricots in thin layers. *Journal of Food Engineering, 55*(3), 209–216.

Verma, L. R., Bucklin, R. A., Endan, J. B., & Wratten, F. T. (1985). Effects of drying air parameters on rice drying models. *Transactions of the ASAE, 28*(1), 296–301.

Vilhena, N. Q., Gil, R., Llorca, E., Moraga, G., & Salvador, A. (2020). Physico-chemical and microstructural changes during the drying of persimmon fruit cv. Rojo Brillante harvested in two maturity stages. *Foods, 9*(7), 870.

Wang, Z., Sun, J., Liao, X., Chen, F., Zhao, G., Wu, J., et al. (2007). Mathematical modeling on hot air drying of thin layer apple pomace. *Food Research International, 40*(1), 39–46.

Yamada, H., Ando, T., Tsutani, K., Amano, S., & Yamamoto, Y. (2009). Mechanism of browning occurring during the processing of semi-dried persimmons. *Journal of the Japanese Society for Horticultural Science, 78*(1), 124–130.

Zhao, C. C., Ameer, K., & Eun, J. B. (2021). Effects of various drying conditions and methods on drying kinetics and retention of bioactive compounds in sliced persimmon. *LWT, 143*, Article 111149.